

Structural and electronic properties of Si_{1-x}Ge_x alloy nanowires

Federico Iori, Stefano Ossicini, and Riccardo Rurali

Citation: *Journal of Applied Physics* **116**, 154301 (2014); doi: 10.1063/1.4898130

View online: <http://dx.doi.org/10.1063/1.4898130>

View Table of Contents: <http://scitation.aip.org/content/aip/journal/jap/116/15?ver=pdfcov>

Published by the [AIP Publishing](#)

Articles you may be interested in

[Crystal facet effect on structural stability and electronic properties of wurtzite InP nanowires](#)

J. Appl. Phys. **115**, 214301 (2014); 10.1063/1.4880742

[Theoretical studies of the passivants' effect on the Si_xGe_{1-x} nanowires: Composition profiles, diameter, shape, and electronic properties](#)

J. Chem. Phys. **139**, 154713 (2013); 10.1063/1.4825196

[Optical absorption modulation by selective codoping of SiGe core-shell nanowires](#)

J. Appl. Phys. **112**, 114323 (2012); 10.1063/1.4768475

[C-doped ZnO nanowires: Electronic structures, magnetic properties, and a possible spintronic device](#)

J. Chem. Phys. **134**, 104706 (2011); 10.1063/1.3562375

[Electronic properties of strained Si/Ge core-shell nanowires](#)

Appl. Phys. Lett. **96**, 143119 (2010); 10.1063/1.3389495



2014 Special Topics

PEROVSKITES

2D MATERIALS

MESOPOROUS MATERIALS

BIOMATERIALS/ BIOELECTRONICS

METAL-ORGANIC FRAMEWORK MATERIALS

AIP | APL Materials

Submit Today!

Structural and electronic properties of $\text{Si}_{1-x}\text{Ge}_x$ alloy nanowires

Federico Iori,^{1,2} Stefano Ossicini,^{1,3} and Riccardo Rurali^{4,a)}

¹Dipartimento di Scienze e Metodi dell'Ingegneria, Centro Interdipartimentale Intermech and En&tech, Università di Modena e Reggio Emilia, via Amendola 2 Pad. Morselli, I-42122 Reggio Emilia, Italy

²European Theoretical Spectroscopy Facility (ETSF) and Institut de Ciència de Materials de Barcelona (ICMAB-CSIC), Campus de Bellaterra, 08193 Bellaterra, Barcelona, Spain

³"Centro S3", CNR-Istituto di Nanoscienze, Via Campi 213/A, 41125 Modena, Italy

⁴Institut de Ciència de Materials de Barcelona (ICMAB-CSIC), Campus de Bellaterra, 08193 Bellaterra, Barcelona, Spain

(Received 27 June 2014; accepted 3 October 2014; published online 15 October 2014)

We present first-principles density-functional calculations of $\text{Si}_{1-x}\text{Ge}_x$ alloy nanowires. We show that given the composition of the alloy, the structural properties of the nanowires can be predicted with great accuracy by means of Vegard's law, linearly interpolating the values of a pure Si and a pure Ge nanowire of the same diameter. The same holds, to some extent, also for electronic properties such as the band-gap. We also assess to what extent the band-gap varies as a function of disorder, i.e., how it changes for different random realization of a given concentration. These results make possible to tailor the desired properties of SiGe alloy nanowires starting directly from the data relative to the pristine wires. © 2014 AIP Publishing LLC.

[<http://dx.doi.org/10.1063/1.4898130>]

I. INTRODUCTION

Semiconducting nanowires (NWs) are recognized as important building blocks for future applications in nanoelectronics.^{1,2} Silicon-Germanium NWs have attracted an increasing interest in recent years, because of the possibility to modulate the electronic and transport properties, not only by changing the size of the system but also by engineering the geometry of the Si/Ge interface or the relative composition of Si and Ge atoms.³

The structural and electronic properties of a nanowire in the quantum confinement regime can be tuned by controlling its size. Random alloys constitute a relative straightforward way to design materials whose properties can be tuned between those of the parent materials by controlling the composition. Therefore, in an alloy nanowire, one can play with both an *extrinsic* size effect and an *intrinsic* alloying effect to achieve the desired properties.⁴ If we consider also doping or the dependence of some properties on the growth orientation, it is easy to understand why SiGe NWs are truly versatile materials for a wide range of applications, including nanoelectronics,^{5,6} photovoltaics,⁷ thermoelectrics,⁸⁻¹⁰ and photonics.^{4,11} A few *ab-initio* calculations of SiGe alloy NWs have been previously published,¹²⁻¹⁶ but they deal with wires of rather small diameters, are mostly related to the role of quantum confinement effect on the electronic structure and do not tackle directly the effect of the composition or of the random nature of the alloy.

In this work, we study to what extent the structural and electronic properties of $\text{Si}_{1-x}\text{Ge}_x$ NWs of arbitrary composition can be predicted from those of the pure Si and Ge NWs of the same diameter. We show that structural properties, such as the lattice parameter and the Young modulus, scale linearly with the Ge content x , while a small *bowing*

parameter induces some non-linearities in the dependence of the band-gap with the composition.

The paper is organized in sections as follows. In Sec. II, we present the computational techniques used to perform the calculations. Section III is devoted to the dependence of the lattice constant on the alloy composition, while in Secs. IV and V we discuss how the electronic properties are affected by alloying and by disorder for different compositions of SiGe NW. Finally, in Sec. VI we report our conclusions.

II. METHODS

The nanowires described in this article have been studied within the Density Functional Theory (DFT) framework in its generalized gradient approximation (GGA-PBE) for the exchange-correlation functional.¹⁷ To study very large system with hundreds of atoms, we used a linear combination of numerical atomic orbitals method as implemented in the SIESTA code.¹⁸ Core electrons have been accounted by means of norm-conserving pseudopotentials taken in their frozen-core formulation, while the one electron wave functions of valence electrons have been described by a linear combination of carefully optimized single- ζ polarized (SZP) basis functions. We study $\text{Si}_{1-x}\text{Ge}_x$ NWs grown along the $\langle 111 \rangle$ axis with diameters of 1.5, 2.1, and 2.5 nm and consider five different compositions: $x=0$ (all-Si NW), 0.25, 0.50, 0.75, and 1.00 (all-Ge NW). H atoms are used to passivate the dangling bonds at the surface of the nanowire. Freestanding NWs are grown through the vapor-liquid-solid method starting from precursor SiH_4 and GeH_4 in their gas phase. Therefore, the H atoms are naturally present in the final state of the NW.³ Additionally, HF attack of the oxidized wires after growth is a well-established method to achieve the removal of the SiO_2 layer and results in individual termination of each dangling bond with a H atom.¹⁹ This passivation preserves the semiconducting electronic character of the

^{a)}Electronic mail: rrurali@icmab.es

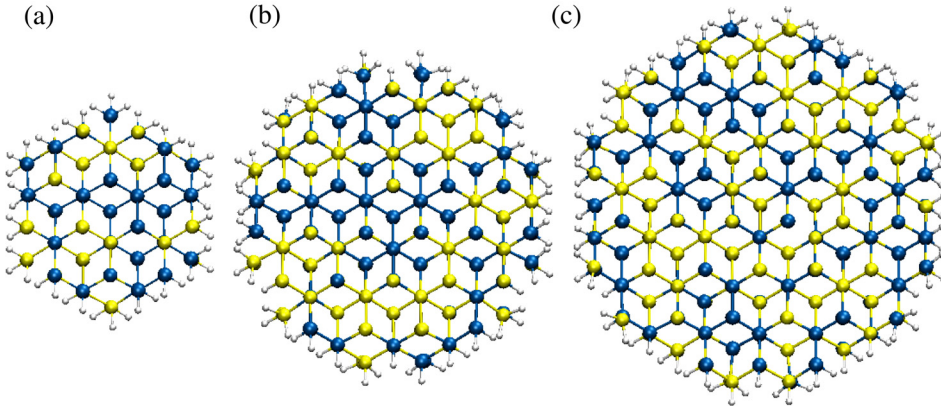


FIG. 1. Cross section view of the (a) 1.5, (b) 2.1, and (c) 2.5 nm diameter $\text{Si}_{1-x}\text{Ge}_x$ NWs for $x=0.5$. Blue, yellow, and white spheres represent Si, Ge, and H atoms, respectively.

freestanding NWs as measured in the experiments, avoiding the formation of spurious electronic states inside the electronic gap of the NW that could lead to a metallic behavior.²⁰ We sample the Brillouin zone with 9 \mathbf{k} -points along the periodic direction of the wire, taken parallel to the z -axis of the crystal cell. A sketch of the wires studied in the case of $x=0.5$ is shown in Fig. 1. A $1 \times 1 \times 2$ and a $1 \times 1 \times 3$ supercells are used to study the variability of the electronics properties (Sec. V). Alloyed configurations are generated by randomly selecting a subset of lattice positions in order to approximately achieve the desired composition.²¹ Compositions are indicated in Table I. The dependence of the properties of the NWs with respect to the specific random realization of a certain composition is discussed in Sec. V.

III. VEGARD'S LAW FOR SiGe ALLOY NANOWIRES

Vegard's law²² is an empirical relation that relates the lattice constant of an alloy with the concentrations of the constituent elements.²³ According to Vegard's rule, then, the lattice constant of a $\text{Si}_{1-x}\text{Ge}_x$ of arbitrary composition x system is given by

TABLE I. Composition of the NWs studied.²¹ Ge concentration x is calculated as $n_{\text{Ge}}/(n_{\text{Si}} + n_{\text{Ge}})$, disregarding the H atoms. For brevity, throughout the text these concentrations are rounded to 0.00, 0.25, 0.50, 0.75, and 1.00.

	n_{Si}	n_{Ge}	n_{H}	x
$d=1.5$ nm	74	0	42	0.00
	56	18	42	0.24
	39	35	42	0.47
	19	55	42	0.74
	0	74	42	1.00
$d=2.1$ nm	170	0	66	0.00
	121	49	66	0.29
	84	86	66	0.50
	39	131	66	0.75
	0	170	66	1.00
$d=2.5$ nm	242	0	78	0.00
	182	60	78	0.29
	120	122	78	0.50
	58	184	78	0.75
	0	242	78	1.00

$$a_{\text{Si}_{1-x}\text{Ge}_x} = (1-x)a_{\text{Si}} + xa_{\text{Ge}}. \quad (1)$$

The validity of Vegard's law for bulk²⁴ and thin film²⁵ SiGe alloy has been demonstrated, but a systematic study for strongly confined systems such as nanowires is still lacking. Our first goal is carrying out an exhaustive scrutiny of the predictive power of Vegard's law to determine the equilibrium axial lattice parameter of $\text{Si}_{1-x}\text{Ge}_x$ NWs of different diameter and Ge concentration by total energy calculations.

As Fig. 2 nicely shows the lattice constant increases linearly with the Ge content x as one goes from an all-Si ($x=0$) to an all-Ge NW ($x=1$) for all the considered wire's diameter, thus Vegard's law holds and can be used to predict the

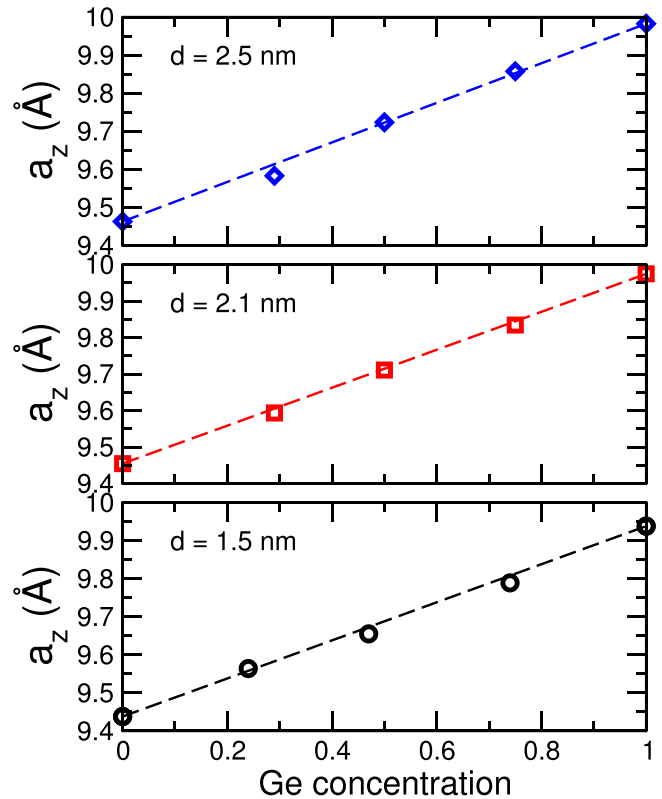


FIG. 2. Calculated equilibrium axial lattice parameter a_z of $\text{Si}_{1-x}\text{Ge}_x$ alloy nanowires with diameters of 1.5, 2.1, and 2.5 nm and an increasing Ge concentration. The dashed lines indicate the prediction based on Vegard's law. Notice that only at thicker diameters the relation $a_z = \sqrt{3}a$, where a is the bulk lattice parameter, will be recovered. Here, for all the diameters investigated and for both Si and Ge we find $a_z < \sqrt{3}a$ (see text).

lattice parameter of an alloy NW of arbitrary composition just knowing the equilibrium lattice parameter of a Si and a Ge NW of the same diameter. The errors committed by direct application of Vegard's law with respect to calculated values are within 0.3%, thus the reliability of these predictions is extremely satisfactory.

It is noteworthy that the axial lattice parameter depends also on the wire diameter. In particular, we have found shorter lattice constants than the bulk counterpart, in agreement with previously published results for Si NWs grown along the same crystal axis.^{2,26} This means that, in principle, the lattice constant should be optimized not only for a composition but also for a given specific diameter. Thanks to the validity of Vegard's law, however, it is enough to have the optimized lattice parameters for Si and Ge NW at different diameters, and the value corresponding to the desired concentration can be simply interpolated.

As for each diameter and concentration we have carried out 10–15 full relaxations at different, fixed lattice constants, by calculating the second derivative of the energy as a function of the strain ϵ we can easily estimate the axial Young's modulus as

$$Y = \frac{1}{V_0} \left. \frac{\partial^2 E}{\partial \epsilon^2} \right|_{\epsilon=0}, \quad (2)$$

where V_0 is the equilibrium volume. The results are shown in Fig. 3 and, although at a closer look somewhat larger errors are committed by straightforward application of Vegard's law, good qualitative predictions can still be made. Values for the 1.5 nm-diameter NW range from 140 to 120 GPa for the all-Si and all-Ge NW, respectively. The thicker wires are stiffer, with values of Y between 180 and 160 GPa, and are very similar, indicating that we have achieved size convergence and reached the bulk limit. Similar results have been reported for $\langle 100 \rangle$ Si NWs²⁷ where Young's modulus saturates at a diameter of ~ 2 nm. Considering that $\langle 111 \rangle$ is the stiffer of the crystallographic axis, our results are consistent with the measured values for bulk Si and bulk Ge, that range between 130 and 190 GPa,^{28–30} and between 100 and 150 GPa,^{28,29,31,32} respectively. They are also in very good agreement with experimental measurements performed

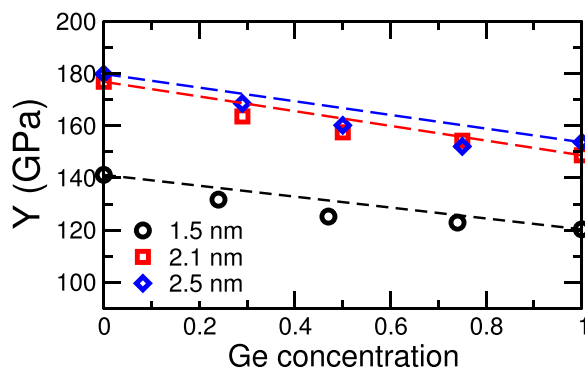


FIG. 3. Calculated Young's modulus of $\text{Si}_{1-x}\text{Ge}_x$ alloy nanowires with diameters of 1.5, 2.1, and 2.5 nm and an increasing Ge concentration. The dashed lines indicate the prediction based on Vegard's law.

directly on Si NWs, where a value of 175 GPa was reported by Hsin *et al.*³³ A good agreement is also obtained with the 106 GPa Young's modulus measured for Ge NWs³² grown along the $\langle 110 \rangle$, which is known to be *softer*.

IV. ELECTRONIC PROPERTIES

Within the quantum confinement regime, the electronic properties of nanowires can be modulated by controlling their diameter, with the band-gap scaling as $d^{-\alpha}$, where d is the wire diameter and α , whose exact value depends on the growth axis, is ~ 1 ($\alpha = 2$ when barrier height is infinite).² Besides this *extrinsic* size effect, common to all kind of strongly confined nanowires, $\text{Si}_{1-x}\text{Ge}_x$ alloy NWs offer the possibility to tune the band-gap by means of an *intrinsic* alloying effect, i.e., by controlling the composition of the system.

All the $\text{Si}_{1-x}\text{Ge}_x$ nanowires considered in this study have an indirect band gap, showing memory of the character of the pure pristine Si and Ge nanowires of the same diameter (see Refs. 34–36). As expected at these diameters, band-gaps are broadened by a strong quantum confinement effect. The calculated direct and indirect band-gaps have been interpolated including a *bowing* parameter, b , as usually done for binary and ternary alloys^{37–39}

$$E_{\text{Si}_{1-x}\text{Ge}_x}^{\text{gap}} = (1-x)E_{\text{Si}}^{\text{gap}} + xE_{\text{Ge}}^{\text{gap}} + x(1-x)b. \quad (3)$$

The band-gaps of the wires (also reported in Table II) as a function of the Ge fraction x are plotted in Fig. 4, together with the interpolation between the values corresponding to $x=0$ and $x=1$, according to Eq. (3). Remarkably, all the bowing factors obtained are very small, particularly those related to the fundamental gaps (see Table III), and the variation of the chemical composition gives still rise to an almost linear reduction of both direct and indirect energy gap as the Ge content increases for all the three diameters considered. This means that the fundamental (indirect) band-gap and the direct band-gap at the Γ point of the largest nanowires can still be predicted with a good accuracy by linearly interpolating the values for all-Si and all-Ge NWs, analogous to what Vegard's law does with structural parameters. This is an important point, because bowing parameters are not known *a priori* and, as can be seen from Table III are strongly diameter dependent. For a linear interpolation, on the other hand, one simply needs the band-gaps of the Si and Ge NW.

TABLE II. Direct and indirect band gaps for the three diameter nanowires.

x	$d = 1.5$ nm		$d = 2.1$ nm		$d = 2.5$ nm	
	Direct (eV)	Indirect (eV)	Direct (eV)	Indirect (eV)	Direct (eV)	Indirect (eV)
0.00	2.92	2.67	2.42	2.11	2.29	1.95
0.25	2.39	2.30	1.76	1.74	1.83	1.62
0.50	2.22	2.14	1.59	1.56	1.57	1.40
0.75	2.08	1.95	1.43	1.36	1.42	1.16
1.00	1.91	1.67	1.30	1.11	1.10	0.94

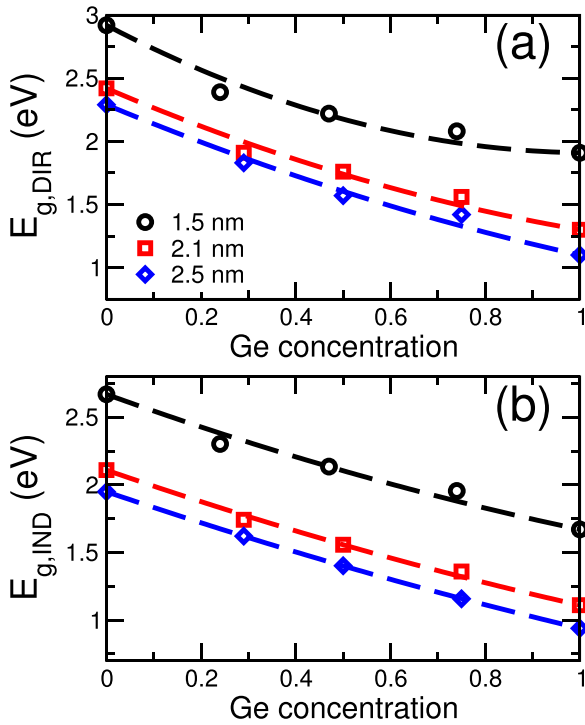


FIG. 4. Trend for the direct gap (panel (a)) and indirect gap (panel (b)) as a function of the Ge composition ratio (x) for different $\text{Si}_{1-x}\text{Ge}_x$ alloy nanowires with diameters equal to 1.5, 2.1, and 2.5 nm. The dashed lines correspond to fits of the data performed according to Eq. (3) of the text.

The only exception is the direct gap of the 1.5 nm NW, with a bowing parameter of 0.96 eV. Predictions based on the interpolation between the all-Si ($x=0$) and all-Ge ($x=1$), neglecting the correction brought by the inclusion of the bowing parameter in Eq. (3), yields errors of 10% and 12% for the case of $x=0.25$ and $x=0.50$, respectively. Fundamental band-gaps follow more closely the linear scaling rule and errors are at most of the order of 5%.

At a given chemical composition, on the other hand, the wires exhibit the well-known quantum confinement effect, with energy gaps that increase when the diameter shrinks from 2.5 down to 1.5 nm.

V. ROLE OF DISORDER

As showed in Sec. IV the electronic properties exhibit some non negligible deviations from an ideally linear interpolation of the band structures of all-Si and all-Ge NWs. In addition to the effects of band-gap bowing, in this section we discuss the variability of the electronic properties of a $\text{Si}_{1-x}\text{Ge}_x$ NW at a certain x for different geometric configurations.¹³ While at fixed x , the structural properties, such as lattice constant and stiffness, are much less sensitive to atomic arrangement randomization and thus can be predicted with

TABLE III. Bowing parameters, b (in eV), obtained by fitting the calculated band-gaps to Eq. (3).

	1.5 nm	2.1 nm	2.5 nm
$E_{g,DIR}$	0.96	0.48	0.36
$E_{g,IND}$	0.26	0.21	0.17

great accuracy on the basis of Vegard's law, the same does not hold for electronic properties.

We tested these ideas in the 2.1 nm $\text{Si}_{1-x}\text{Ge}_x$ NW, where we studied the effect of the disorder and randomization of the SiGe alloy. We generated five fully random alloy configurations for the three different values of the Ge concentration, i.e., $x=0.25$, 0.5, and 0.75. We fully relaxed each of these 15 configurations and calculated the band-structure. As it can be seen in Fig. 5, the band-gap of a $\text{Si}_{1-x}\text{Ge}_x$ NW can vary up to 50 meV from one configuration to the other. Notice that the number of Ge atom in each of the five realizations of a given concentration is exactly the same and only the (random) distribution changes.

In an attempt to correlate the band-gap width with the atomistic structure of the nanowire, we have calculated the average radial coordinate \bar{r}_{Ge} that accounts for the spatial distribution of all Ge atoms inside the nanowire. If r_0 is the average radial coordinate of all the wire lattice sites, $\Delta r_{Ge} = r_{Ge} - r_0$ is a measure of the radial distribution, with $\Delta r_{Ge} > 0$ indicating Ge atoms on average closer to the surface, and with $\Delta r_{Ge} < 0$ indicating Ge atoms located in the innermost part of the wire. Although it is not possible to draw a strict connection between the distribution of the Ge atoms and the resulting band-gap width, some loose correlation seems to exist with the average radial coordinate r_{Ge} of the Ge atoms. Hence, systems with more Ge in the innermost part of the wire have smaller gaps (negative Δr_{Ge} , configuration #5 of $x=0.25$), while large gaps are more frequently associated with Ge atoms that occupy lattice sites that are on average closer to the surface (positive Δr_{Ge} , configurations #2 and #5 of $x=0.25$, or configuration #5 of $x=0.75$).

This crude approach obviously neglect other important factors such as local clustering of Ge atoms, thus it has to be taken qualitatively.

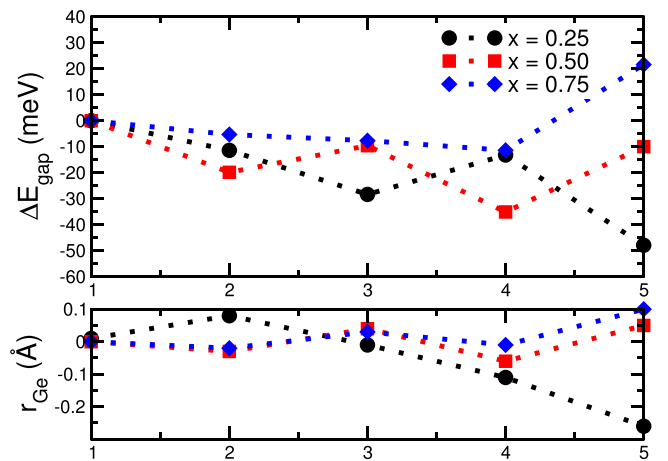


FIG. 5. (Top) Fundamental band-gap of five different $\text{Si}_{1-x}\text{Ge}_x$ NWs with fixed 2.1 nm diameter and for $x=0.25$, 0.50, and 0.75. Given a composition, the five random realization features exactly the same number of Ge atoms and only differ for the Si and Ge spatial distribution on the wire's lattice sites. ΔE_{gap} is the variation of the band-gap with respect to the first configuration, which we have taken as a reference. (Bottom) Average radial coordinate of Ge atoms referred to the average radial coordinate of all the wire's lattice sites. Ge atoms close to the surface contribute with a positive Δr_{Ge} , while Ge atoms close to the wire's core have a negative Δr_{Ge} .

VI. CONCLUSIONS

In conclusions, we have shown that it is possible to modulate the structural and the electronic band structures of $\text{Si}_{1-x}\text{Ge}_x$ alloy NWs continuously between the values of the corresponding pure Si and Ge NWs by varying the composition. Especially for what concerns an important structural parameter such as the lattice constant, Vegard's law provides estimates for an alloy wire of arbitrary composition of very high accuracy. Young's modulus and electronic band-gap are prone to somewhat larger errors, though reliable qualitative prediction can still be made. The band-gap has a mild, but non-negligible dependence on the spatial distribution of the atoms composing the alloy and wires with the same concentration, but different random realizations, can have gaps that differ up to 50 meV.

ACKNOWLEDGMENTS

We acknowledge funding under Contract Nos. FEDER-FIS2012-37549-C05-05 and CSD2007-00041 of the Ministerio de Economía y Competitividad (MINECO). We thank the Centro de Supercomputación de Galicia (CESGA) for the use of their computational resources. F.I. acknowledges support from "Borsa di Studio per la Fisica Edison in memoria di Francesco Somaini" funded by Edison and sponsored by Centro di cultura scientifica "Alessandro Volta" (Italy).

¹D. K. Ferry, *Science* **319**, 579 (2008).

²R. Rurali, *Rev. Mod. Phys.* **82**, 427 (2010).

³M. Amato, M. Palummo, R. Rurali, and S. Ossicini, *Chem. Rev.* **114**, 1371 (2014).

⁴J.-E. Yang, C.-B. Jin, C.-J. Kim, and M.-H. Jo, *Nano Lett.* **6**, 2679 (2006).

⁵J. Xiang, W. Lu, Y. Hu, H. Yan, and C. M. Lieber, *Nature* **441**, 489 (2006).

⁶D. C. Dillen, K. Kim, E.-S. Liu, and E. Tutuc, *Nat. Nanotechnol.* **9**, 116 (2014).

⁷M. Amato, S. Ossicini, and R. Rurali, *Nano Lett.* **11**, 594 (2011).

⁸M. C. Wingert, Z. C. Y. Chen, E. Dechaumphai, J. Moon, J.-H. Kim, J. Xiang, and R. Chen, *Nano Lett.* **11**, 5507 (2011).

⁹E. K. Lee, L. Yin, Y. Lee, J. W. Lee, S. J. Lee, J. Lee, S. N. Cha, D. Whang, G. S. Hwang, K. Hippalgaonkar, A. Majumdar, C. Yu, B. L. Choi, J. M. Kim, and K. Kim, *Nano Lett.* **12**, 2918 (2012).

¹⁰M. Amato, S. Ossicini, and R. Rurali, *Nano Lett.* **12**, 2717 (2012).

¹¹C.-J. Kim, H.-S. Lee, Y.-J. Cho, J.-E. Yang, R. R. Lee, J. K. Lee, and M.-H. Jo, *Adv. Mater.* **23**, 1025 (2011).

¹²M. Amato, M. Palummo, and S. Ossicini, *Phys. Rev. B* **79**, 201302 (2009).

¹³M. Amato, M. Palummo, and S. Ossicini, *Phys. Rev. B* **80**, 235333 (2009).

¹⁴M. Palummo, M. Amato, and S. Ossicini, *Phys. Rev. B* **82**, 073305 (2010).

¹⁵J.-S. Park, B. Ryu, and K. J. Chang, *J. Phys. Chem. C* **115**, 10345 (2011).

¹⁶M. Amato, M. Palummo, and S. Ossicini, *Mater. Sci. Eng., B* **177**, 705 (2012).

¹⁷J. P. Perdew, K. Burke, and M. Ernzerhof, *Phys. Rev. Lett.* **77**, 3865 (1996).

¹⁸J. M. Soler, E. Artacho, J. D. Gale, A. García, J. Junquera, P. Ordejón, and D. Sánchez-Portal, *J. Phys.: Condens. Matter* **14**, 2745 (2002).

¹⁹D. D. Ma, C. S. Lee, F. C. K. Au, S. Y. Tong, and S. T. Lee, *Science* **299**, 1874 (2003).

²⁰R. Rurali and N. Lorente, *Phys. Rev. Lett.* **94**, 026805 (2005).

²¹A Si atom is substituted with a Ge with a probability equal to the desired concentration x . Because of the inherently stochastic nature of this process, the obtained Ge concentrations are very close, but only approximately equal to the target value of x , e.g., 0.25, 0.50, and 0.75.

²²L. Vegard, *Z. Phys.* **5**, 17 (1921).

²³Strictly speaking an alloyed system is no longer periodic, because of the disorder, and in principle, it makes no sense speaking about its lattice parameter. For what computational modeling is concerned, however, the system is typically described within periodic boundary conditions and periodicity is artificially imposed.

²⁴S. de Gironcoli, P. Giannozzi, and S. Baroni, *Phys. Rev. Lett.* **66**, 2116 (1991).

²⁵E. Kasper, A. Schuh, G. Bauer, B. Holländer, and H. Kibbel, *J. Cryst. Growth* **157**, 68 (1995).

²⁶M.-F. Ng, L. Zhou, S.-W. Yang, L. Y. Sim, V. B. C. Tan, and P. Wu, *Phys. Rev. B* **76**, 155435 (2007).

²⁷B. Lee and R. E. Rudd, *Phys. Rev. B* **75**, 041305(R) (2007).

²⁸J. Wortman and R. A. Evans, *J. Appl. Phys.* **36**, 153 (1965).

²⁹E. Borch, S. D. Gennaro, R. Macii, and M. Zoli, *J. Phys. D* **21**, 1304 (1988).

³⁰M. Hopcroft, W. Nix, and T. Kenny, *J. Microelectromech. Syst.* **19**, 229 (2010).

³¹H. J. McSkimin, *J. Appl. Phys.* **24**, 988 (1953).

³²D. A. Smith, V. C. Holmberg, D. C. Lee, and B. A. Korgel, *J. Phys. Chem. C* **112**, 10725 (2008).

³³C.-L. Hsin, W. Mai, Y. Gu, Y. Gao, C.-T. Huang, Y. Liu, L.-J. Chen, and Z.-L. Wang, *Adv. Mater.* **20**, 3919 (2008).

³⁴P. W. Leu, B. Shan, and K. Cho, *Phys. Rev. B* **73**, 195320 (2006).

³⁵R. Rurali, B. Aradi, T. Frauenheim, and A. Gali, *Phys. Rev. B* **76**, 113303 (2007).

³⁶M. Bruno, M. Palummo, A. Marini, R. Del Sole, V. Olevano, A. N. Kholod, and S. Ossicini, *Phys. Rev. B* **72**, 153310 (2005).

³⁷J. A. Van Vechten and T. K. Bergstresser, *Phys. Rev. B* **1**, 3351 (1970).

³⁸M. Ferhat, J. Furthmüller, and F. Bechstedt, *Appl. Phys. Lett.* **80**, 1394 (2002).

³⁹S. Sant, S. Lodha, U. Ganguly, S. Mahapatra, F. O. Heinz, L. Smith, V. Moroz, and S. Ganguly, *J. Appl. Phys.* **113**, 033708 (2013).